Theoretical Aspects of Chemical Reactivity
A. Toro-Labbé (Editor)

Chapter 5

Understanding and using the electron localization function

[a]Patricio Fuentealba, [b]E. Chamorro, and [b]Juan C. Santos

[a]*Departamento de Física, Facultad de Ciencias, Universidad de Chile, Las Palmeras 3425, Casilla 653 and*
[b]*Departamento de Ciencias Químicas, Facultad de Ecología y Recursos Naturales, Universidad Andrés Bello, Av. República 275, Santiago, Chile*

1. Introduction

The applications of quantum mechanics to chemistry have primordially two goals. First, to provide the numerical value of observables which can be confronted with experimental measurements and, second, to help in understanding many empirical concepts widely used in chemistry. The electron localization function, ELF, enters in the second goal. It helps in understanding the empirical concept of electron localization, specially the pair electron localization in the spirit of Lewis structures. This paper is not an attempt to review all of the applications of the ELF, rather the aims are to explain in an easy way with as less as possible of mathematical formalism the significances of the ELF and, more important, how to use it. Hence, from the very beginning, we give answer to a common question of chemists in front of theoretical paper: Why should I bother trying to understand this function, when I do not have any chance to apply it and when I do not have any software to calculate it? Well, in this case, everybody can calculate the ELF using the TOPMOD software developed by Silvi and co-workers[1] which is free. It uses the output of popular programs for electronic structure calculation, i.e. the commercial package of programs GAUSSIAN[2] and the free software GAMMES[3] to obtain the ELF and elaborate the necessary topological analysis. The ELF is also implemented in some other packages designed for periodic systems[4] or can also be calculated using the interfacing program DGRID[5] for GAUSSIAN,[2] MOLPRO[6] and ADF.[7] A new algorithm to fast calculation of the 3D and 2D arrays needed for the topological analysis of ELF is also available.[8]

The ELF was introduced by Becke and Edgecombe[9] and first applied to a great range of systems, from atoms to molecules and solids, by Savin et al.[10] Some years later, Silvi

and Savin[11] proposed a topological classification and rationalization of the ELF which helps in giving a quantification of the chemical concepts associated with the function. After that, and with the launch of the TOPMOD[1] free software, there have been many applications of the ELF to molecules, clusters and solids.

One of the key concepts to understand the significance of the electron localization is the Fermi hole, which is a direct consequence of the Pauli exclusion principle.[12] It permits to answer the difficult question pointed out by Lewis[13] when he introduced in chemistry the concept of the electron pair. His question is as follows: If the only law of nature acting on the electron's movement is the Coulomb's law which is repulsive between a pair of electrons, then how is it possible to find a pair of electrons moving together in a certain region of space? In fact, Lewis postulated the failure of the Coulomb's law for small distances. Remember that at this time the quantum mechanics was not fully understood, and later, Lewis changed his position. In fact, it is important to notice that, in a rigorous sense, it does not make any sense to talk about a localized electron because it goes against the Heisenberg's uncertainty principle. A nice explanation to all of this is given by Bader,[14] and we follow it. The existence of a localized electron pair implies that there exists a high probability of finding two electrons of opposite spin in a given region of the space and for which there is a small probability of exchange with other electrons that are outside of this region. To understand this, it is necessary to think that as an electron moves through space, it moves also with its Fermi hole. The Fermi hole related to a given electron in a given position in the space is a distribution function which measures the decrease due to the Pauli principle in the probability of finding another electron of the same spin at some position in the space. Hence, it depends on the position of the reference electron, say $\vec{r}_1$, and on the position of the other electron, say $\vec{r}_2$. Therefore, for a given spin, the diagonal of the Fermi hole, $\vec{r}_1 = \vec{r}_2$, should be equal to the total density for the given spin at this point. This is the only way to be sure that the probability of finding another electron of the same spin at this position is zero, condition necessary to respect the Pauli principle. For the same reason, for a fixed $\vec{r}_1$, the position of the reference electron, the integration of the Fermi hole over $\vec{r}_2$ corresponds to the removal of one electron of identical spin. Hence, the Fermi hole describes the spatial delocalization of the charge of the reference electron. As written by Bader, 'an electron can go only where its hole goes and, if the Fermi hole is localized, then so is the electron'. One example: an electron of a given spin moving near a nucleus. There is a big attractive potential acting on the electron, and the potential well to get outside this region is also big. Its Fermi hole is strongly localized around this region of the space. Suppose now that the Fermi hole is so localized on this region that everywhere on this region it equals its maximum value, the total density of the given spin, then, all other electrons of this spin are completely excluded from this region. The same result would be obtained for an electron of the other spin if it happens to be in the same region of the space. Hence, this pair of electrons of different spin is confined to move on this particular region of the space in the vicinity of a nucleus where all the other electrons irrespective of its spin are excluded. Since repulsions between the electrons act in opposition to this effect, the localization can never be perfect. It is important to notice that the Fermi hole does not produce an attraction between a pair of electrons of different spin, it rather produces an extra repulsion between the pair of electrons and all the rest. In general, this argumentation is correct for the inner $1s^2$ pair of electrons, and may be for the core electrons of any system, but it is clearly difficult to apply to the

valence electrons which are weakly bonded. Therefore, it is important to have in mind that the image of localized electrons in a bond or as a lone pair are only good models in order to understand the chemistry, but they do not have any physical realization.

In the next section, the principal ingredients involved in the ELF will be explained, and their relation with chemical concepts will be clarified. Then, a brief comparison of the ELF with other theoretical related tools, like the atoms in molecules model of Bader, will be done. Next, some elementary concepts from the mathematical theory of topological analysis will be in a rather crude way presented. After that, some applications, extensions and results will be discussed, focusing in particular on applications developed at our group.

2. ELF developments

2.1. Becke's proposal and interpretation

In studying the correlation among electrons, it was very early realized that because of the Pauli principle the movement of electrons of the same spin is strongly correlated than the one between electrons of different spin. Therefore, it seems convenient to study the electron pair density for electrons of the same spin and for electrons of different spin, separately. The electron pair density, $\rho_2^{\sigma\sigma'}(\vec{r}_1, \vec{r}_2)$, gives us the probability of finding an electron of spin σ at point $\vec{r}_1$ when a second electron of spin σ' is located at point $\vec{r}_2$. Because the electron–electron interaction depends only on the distance between the electrons and not on the angular orientation, it is convenient to change the coordinate system to the ones defined by $\vec{r} = ½(\vec{r}_1 + \vec{r}_2)$ and $\vec{s} = \vec{r}_1 - \vec{r}_2$. The advantage of the new coordinate system is that now the electron interaction does not depend on six variables ($\vec{r}_1$ and $\vec{r}_2$) but only on four ($\vec{r}$ and s). Hence, only the spherical average electron pair density is necessary. This is defined as

$$\rho_2^{\sigma\sigma'}(\vec{r}_1, s) = \frac{1}{4\pi} \int \rho_2^{\sigma\sigma'}(\vec{r}_1, s) \mathrm{d}\Omega_s, \tag{1}$$

where the integration is over the angles of the vector $\vec{s}$.

Now, Becke and Edgecombe[2] preferred to work with the conditional pair density for electrons of the same spin which is a measure of the conditional probability of finding an electron at position $\vec{r}_2$ when with certainty there is an electron of the same spin at position $\vec{r}_1$. It is given by

$$P^{\sigma\sigma}(\vec{r}, s) = \frac{\rho_{2,av}^{\sigma\sigma'}(\vec{r}, s)}{\rho_\sigma(\vec{r})} \tag{2}$$

where $\rho_\sigma(\vec{r})$ is the electron density of electrons with spin σ which in the Kohn–Sham approximation is given by

$$\rho_\sigma(\vec{r}) = \sum_i^\sigma \phi_i(\vec{r})^2 \tag{3}$$

with the Kohn–Sham orbitals given by the set $\{\phi_i\}$, and the sum is over all the occupied orbitals with spin σ.

Then, they proposed to examine the Taylor series expansion of the spherical average conditional pair density in the vicinity of the point $s = 0$ where one is measuring the short-range behaviour of the electron at point $\vec{r}_2$ approaching the reference point $\vec{r}_1$. The leading term of the Taylor series expansion is given by

$$P^{\sigma\sigma}(\vec{r}, s) = \frac{1}{3}(\tau_\sigma - \frac{1}{4}\frac{(\nabla\rho_\sigma)^2}{\rho_\sigma})s^2 + \cdots\cdots, \tag{4}$$

where τ_σ is the positive definite kinetic energy density defined by

$$\tau_\sigma = \sum_i^\sigma (\nabla\phi_i)^2. \tag{5}$$

After Becke and Edgecombe, the Taylor expansion contains all the electron localization information. The smaller the probability of finding the second electron near the point $\vec{r}$ the more localized is the reference electron. Hence, electron localization is directly related to the bracket enclosed in the right hand side of (4)

$$D_\sigma = \tau_\sigma - \frac{1}{4}\frac{(\nabla\rho_\sigma)^2}{\rho_\sigma}, \tag{6}$$

which is a non-negative quantity.[15] One can also easily demonstrate that D_σ vanishes for the hydrogen atom and also for the helium atom in the Hartree–Fock (HF) approximation, and it is also expected to be negligible in the regions near the nuclei, where one finds the most localized electrons.

Therefore, it is reasonable to expect that the quantity D_σ will be small in the regions of the space where the probability of finding a localized electron or a localized pair of electrons is high. However, the function D_σ can have very high values in other places, and one does not know how near to zero should be to consider an electron to be localized. Hence, Becke and Edgecombe proposed two additional scaling rules. The homogeneous electron gas, the kinetic energy density of which is given by $D_\sigma^0 = c_f\rho^{5/3}$, is used as a reference, and for numerical convenience the function is mapped to one which is defined between zero and one. Hence, they proposed the following ELF:

$$\mathrm{ELF} = (1 + \chi_\sigma^2)^{-1}, \tag{7}$$

where

$$\chi_\sigma = D_\sigma / D_\sigma^0. \tag{8}$$

In this way, the following inequality is obeyed

$$0 \leq \mathrm{ELF} \leq 1 \tag{9}$$

and a value of the ELF close to one corresponds to a region of the space where there is a high probability of finding electron localization, whereas an ELF value close to one-half corresponds to a region of electron gas-like behaviour. The so defined function is independent of any unitary transformation of the orbitals, and, in principle, it is

derivable from the electron density. In fact, it is only necessary to have ones of the currently used procedures to obtain the Kohn–Sham potential from the density to get from the potential, via the Kohn–Sham equations, the necessary orbitals to calculate the function τ_σ as it was done by Kohout and Savin.[16] Moreover, the function can be, in the same indirect way, computed from the experimentally obtained density. There have been approximate determinations of the ELF using electron densities derived from X-ray diffraction data,[17] and also slight modifications of the ELF to bypass the use of orbitals. They have also the interesting property of relating the ELF to other physical concepts. The first one[18] proposed to use the sum rule for the exchange hole to model directly the pair conditional probability. Other used an approximate kinetic energy functional to relate the ELF to the electrostatic potential[19] and, finally, the ELF has also been related to the concept of electronic temperature.[20] This connection between local temperature and electron localization has been recently reviewed.[21] We should also mention the recently introduced electron localizability indicator (ELI),[22] based on a functional of the same-spin pair density which is related to the ELF within an HF approximation, and it differs from the ELF in the case of correlated wave functions.

2.2. Savin's interpretation

The so presented ELF is mainly based on an interpretation of the conditional pair probability density for electrons of the same spin. A conceptually different interpretation was put forward by Savin et al.[23] who realized that the term D_σ could be generalized for any density ρ independent of the spin as

$$D = \frac{1}{2}\sum_i (\nabla\phi_i)^2 - \frac{1}{8}\frac{(\nabla\rho)^2}{\rho}. \tag{10}$$

One can easily verify that for a closed-shell system, both expressions are the same. The main point now is to recognize the second term of the right hand side of the last equation as the von Weizsacker kinetic energy density,[24] which is exact for the hydrogen atom, exact for the helium atom in the HF approximation and exact for a system of bosons. Remember that boson particles can occupy all of them the same quantum state being in this case the perfect localization. The first term of the right hand side represents the kinetic energy density of the molecule under study. Hence, in the region of the space where there is a high probability of finding a localized electron pair, the von Weizsacker kinetic energy density will be a good model, and the function D will have a value near zero. Within this interpretation, the ELF is formally a measure of the excess of kinetic energy density due to the Pauli exclusion principle. Now, it should be clear that the concept of electron pair localization is nothing else but a manifestation of the Pauli exclusion principle.

2.3. Numerical stability

One important characteristic of the ELF is its numerical stability with respect to the theoretical level at which the electron density and the molecular orbitals have been

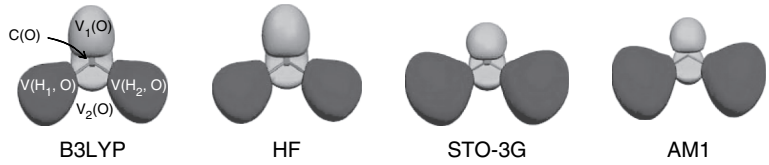

Figure 1 H_2O isosurfaces calculated at different levels of theory

calculated. Contrary to most of the population analysis that depend seriously on the basis set used or the method of calculation (HF, BLYP, B3LYP, etc.), the ELF is rather independent of these changes. As an example, one can see in Figure 1 an isosurface of the ELF for the water molecule calculated at different levels, from AM1 semiempirical method to some of the currently used functionals with a relative big basis set (6-311++G**). The qualitative view of the picture is in all cases the same. Hence, the chemical interpretation of the ELF is also the same. Indeed, there are a series of works where the ELF has been calculated, specially for solids, using en extended Hückel method.[25,26]

This good property of the ELF can be at first glance explained looking at the qualitative behaviour of the total electron density, which is also very independent of the level of calculation. Of course the numerical values can be different, so are the expectation values based on the density. But the maxima and minima are all almost at the same positions. More precise, all the critical points are almost at the same positions. Next, it will be shown that mathematically this means that the function is topologically invariant to the level of calculation.

Burdett and McCormick gave a more precise explanation to this invariance.[27] They concluded that the ELF is primordially based on the nodal properties of the occupied orbitals of the system. Hence, what matters is the symmetry of the orbitals which is independent of the level of calculation. According to this view, electrons are localized in regions of the space where there are significant electron density and few nodes from all of the occupied orbitals. The number of nodes is also important in order to understand the ELF for transition metals, as it will be shown later.

2.4. Analogies and differences with the atoms in molecules (AIM) model

The atoms in molecules (AIM) model of a molecule proposed by Bader[14] is completely based on the properties of the electron density. The maxima and minima of the density are used to define a volume in the space, which can be associated with a particular atom in a molecule. Notice that such *atoms in a molecule* are clearly not spherical, and they extend over all the space with sharp boundaries between two atoms. The information about the zones of depletion or accumulation of charge is extracted from the Laplacian of the density, $\nabla^2\rho(\vec{r})$. The Laplacian of a function determines where the function will locally augment its value, $\nabla^2\rho(\vec{r}) < 0$, and where it will decrease its value, $\nabla^2\rho(\vec{r}) > 0$. This cannot be made using just the density because the density is a monotonically decreasing function. Hence, the regions of the space where $\nabla^2\rho(\vec{r}) < 0$

represent the regions of charge concentration. Bader preferred to work with the negative of the Laplacian, $-\nabla^2\rho(\vec{r})$, so that a maximum of this function denotes a position at which the electron density is maximally concentrated. It has been found that the local maxima of the function correspond very well to the regions of bonding according to the VSEPR model of Gillespie.[28] Hence, the regions of charge concentration defined by the Laplacian of the electron density correspond to the regions of space dominated by the presence of a single pair of electrons. In this sense, one can think that both functions, the ELF and the negative of the Laplacian of the electron density, have the same information. Bader et al.[29] have done an extensive study of the topological characteristics of both functions. They found that, in general, both functions are homeomorphic, it means that in all the studied cases both functions present the same number of maxima and minima and they are located almost on the same regions. However, there are systematic differences. In all cases, the radial distance from a nucleus at which the maxima of the ELF is found is always greater than in the negative of the Laplacian of the electron density, and, more important, for a single covalent bond the ELF presents a clear region of the space between both atoms with the only exception of bonds to hydrogen, whereas the negative of the Laplacian of the electron density yields to separate regions associated with each of the participating atoms, and it does not give a clear visualization of the simple covalent bond. In a later work, Bader and Heard[30] concluded that the ELF has no direct relationship to the conditional pair density for same-spin electrons. Hence, it seems reasonable to use both functions as complementary tools. As an example, Llusar et al.[31] used both functions to study the metal–metal bond in a series of dimers and complexes, and Chesnut and Bartolotti[32] used also both functions to study the aromaticity in some substituted cyclopentadienyl systems. More recent examples include the study of unusual bonding in some Bismuth-bridged binuclear molybdocene complexes,[33] the nature of bonding in the Leflunomide and some of its biological active metabolites,[34] the reactivity of hydroxyperoxy radical,[35] the bonding in the singlet and triplet gas-phase ion/molecule reactions of NbO_3^-, NbO_5^-, and $NbO_2(OH)_2^-$ with O_2,[36] the absorption of Pd on MgO(0 0 1), α-Al_2O_3(0 0 0 1) and SiO_2 surfaces,[37] the bonding interactions metal-carbonyl,[38] the gas-phase acidity of some oxyacids[39] and the nature of bonding of the three-centre-four-electron bond.[40]

2.5. Results in atoms

As a first example of how the ELF works, some results in atoms are presented. Although in the original paper, Becke and Edgecombe[9] presented results for some atoms, it was the work of Kohout and Savin[41] which showed all the potential of the ELF in explaining the atomic electron structure. The electrons occupying orbitals with the same principal quantum number define each atomic shell, and the concept is primordial to explain the periodic properties. However, it is not so clear from the theoretical point of view. The electron density alone does not show any shell structure, it decays exponentially. It is necessary to use the radial distribution $4\pi r^2\rho(\vec{r})$ to see the atomic shell structure.[42,43] However, it fails for the heavier atoms. On the other side, the ELF is not only able to show the shell structure but is also able to give the radius of each shell r^s and the amount of electrons q^s on each shell.[20] The maxima of the ELF indicate the shells. They are separated by the minima of the ELF which are the radius of each shell. The number of

Table 1 The ELF shell radii and electron numbers

	qk	rk	q^{L}	r^{L}	q^{M}	r^{M}
Li (^{2}S)	2.0	1.53	1.0			
F (^{2}P)	2.1	0.34	6.9			
Na (^{2}S)	2.2	0.26	7.9	2.14	1.0	
Cl (^{2}P)	2.2	0.15	7.9	0.82	6.9	
Cr (^{7}S)	2.2	0.10	8.0	0.47	12.3	2.37
Cu (^{2}S)	2.2	0.08	8.3	0.36	17.2	2.17
Br (^{2}P)	2.2	0.07	8.5	0.28	17.2	1.10

electrons in each shell is calculated by the numerical integration of the electron density between the boundaries of the shell. In Table 1, some representative results are shown. One can see that always the innermost K-shell has around two electrons, the following shell, the L-shell, has almost always around eight electrons with systematic deviations for the heavy atoms. Kohout and Savin[41] concluded that the ELF is able to resolve the atomic shell structure for all atoms from Li to Sr, and it also gives for each shell electron numbers close to those given by the periodic table of the elements. Small deviations were also explained due to the influence of core-valence separation, especially when *d* electrons are present.[44]

In Figure 2, the ELF curves for some selected atoms are depicted. Here, one can use the spherical symmetry to plot it as a function of only one variable, the distance to the nuclei. It is interesting to note that for the alkaline metal atoms the ELF does not decay to zero when the distance goes to infinity. The same fact occurs for the alkaline-earth-metal atoms and for any spherical system with an outer shell formed only by electrons on s-orbitals. In fact, for the hydrogen atom, the ELF is equal to one everywhere. On the other side, one can perfectly see the shell structure even for rubidium atom. The same is true for the noble gas atoms and, as shown by Kohout and Savin,[22] for all the atoms to Sr.

2.6. Topological tools

The ELF is a scalar function of three variables, and in order to obtain more information from it, it is necessary to use a mathematical approach called differential topology analysis. This was first done by Silvi and Savin,[11] and later on extended by them and co-workers.[45,46] Unfortunately, one cannot visualize in a global way a three-dimensional function. Usually, one resorts to isosurfaces like the ones in Figure 1, or to contour maps. A three-dimensional function has a richer structure than a one-dimensional function, and their mathematical characterization introduces some new words which are necessary to understand in order to go further. It is the purpose of this section to explain this new terminology in a manner as simpler as possible. Let us begin with a one-dimensional (1D) example, a function $f(x)$ like the one in Figure 3. The function has three maxima and two minima characterized by the sign of the second derivative. In three dimensions (3D) there are more possibilities, for there are nine second derivatives. Hence, one does not talk about maxima but about *attractors*. In 1D, the attractors are points, in

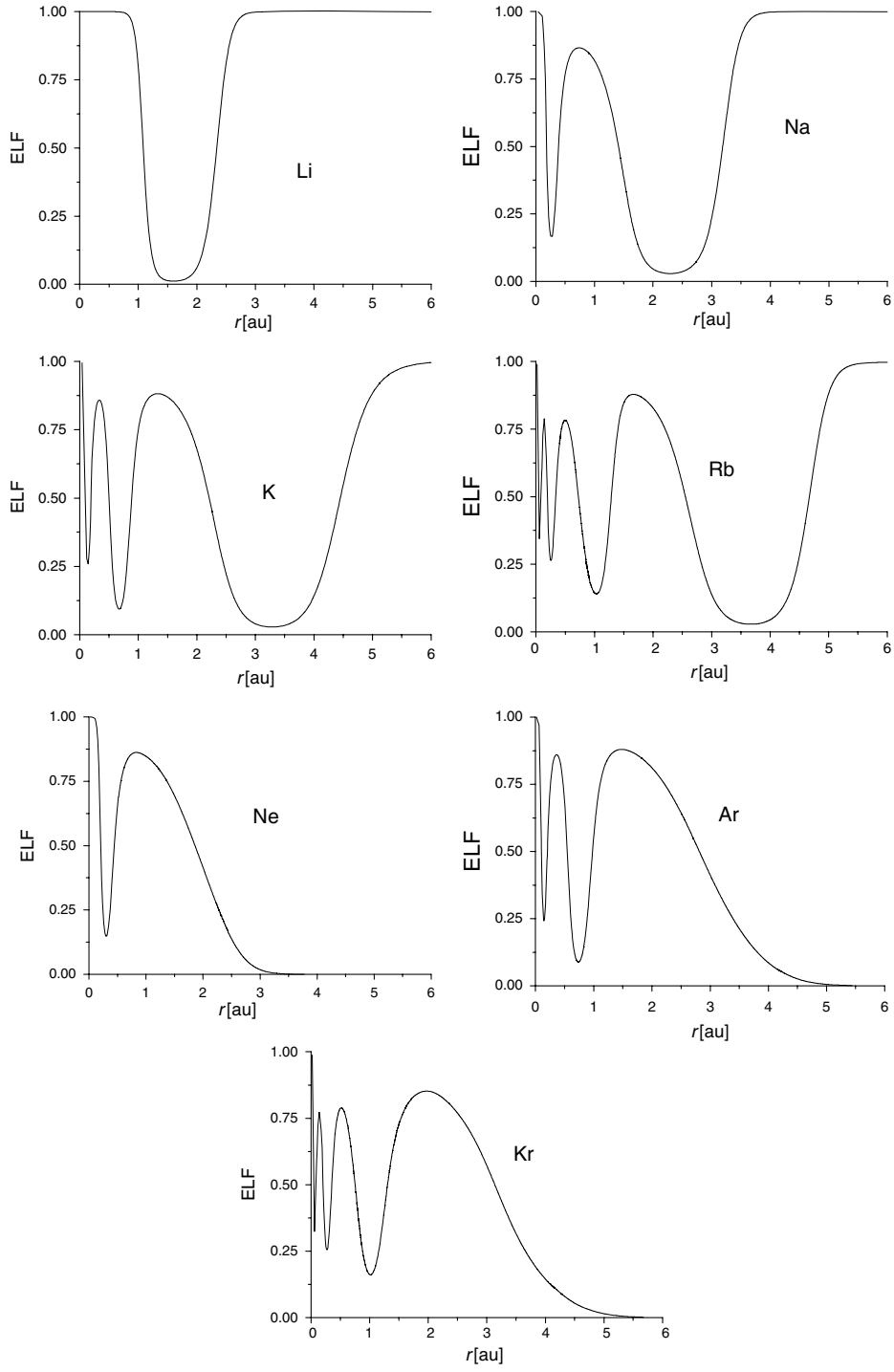

Figure 2 The atomic shell structure determined by ELF

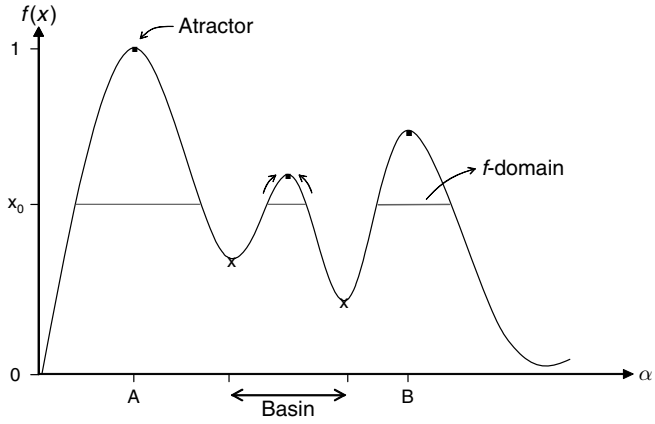

Figure 3 Localization domains of $f(x)$

3D they can be a point, a surface or a volume, so are also the minima. In 1D, every attractor is surrounded by two minima (suppose the limit values at zero and infinity are minima), which encloses a line (see Figure 3); in 3D they are surrounded by a surface that encloses a volume. In 1D, mathematically one characterizes the *basins* saying that it is the line formed by all the points around the attractor such that the point plus the first derivative is closer to the attractor. In 3D, one follows the gradient of the function saying that the basin is formed by all the points enclosed in the volume formed by the gradient lines ending up in the attractor. One can try to visualize it: look at the 1D function in Figure 3, rotate around the y - axes in 360° and you will have a 2D function and the basin indicates in the Figure 3 will be a surface. One more rotation will produce a 3D function and the basin will be a volume. The concept of isosurface has also its correspondence in 1D. Look in Figure 3 at the points where the function has the value $f(x) = x_0$. The lines joining the points are the equivalent to the volume enclosed by an isosurface. They are called the *f-domain*. In Figure 3 there are three *f-domains* at $f(x) = x_0$. However, if one goes to a lower value of the function, close to $f(x) = 0$, one will have only one *f-domain*. There is an important difference in both cases. In the first case, at $f(x) = x_0$, the *f-domains* enclose only one attractor each, but in the second case, close to $f(x) = 0$, the only *f-domain* encloses the three attractors.

The *f-domains* are said to be *reducible* when they contain more than one attractor and *irreducible* when they contain one attractor. The basins formed by the irreducible *f-domains* have a clear chemical meaning and mathematical characterization. There are basically two types of basins.[45] If the basin contains a nucleus (except a proton) it is a core basin (C). Otherwise it is a valence basin (V). Always a valence basin will be connected with at least one core basin. A basin representing a lone electron pair will be connected with only one core basin and its attractor will be called monosynaptic. A basin representing a covalent bond will be connected with two core basins, and its attractor will be called disynaptic. There are also higher synaptic orders. Hydrogen is a particular case because it does not have core electrons. Therefore, it is an exception. The bond of any atom to hydrogen appears as a basin that contains the proton and, in general they have a great volume. Silvi has recently discussed the usefulness of the synaptic order concepts in the context of multicentre bonding analysis.[47] For the

graphical visualization, it is convenient to have a colour code associated with each type of basin. For example, in the water molecule (Figure 1) there is one core basin for the oxygen K-shell denoted C(O) of violet colour. Two basins containing the protons and associated with the O–H bond are denoted $V(H_1, O)$ and $V(H_2, O)$ and they are blue in colour, and there are two basins corresponding to the lone pairs $V_1(O)$ and $V_2(O)$ yellow in colour.

In the last example, it is clear that a graphical representation of the ELF is able to give a qualitative picture of the type of bonds in a molecule and the regions of the space where it is possible to find electron pairs. However, this is only qualitative information. To get a more quantitative knowledge about the localization one has to go to the integrated density and other properties.[45] Remember that in the atomic case the integration of the electron density between two minima of the ELF yields the number of electrons on each shell. Using the new terminology, we have integrated the electron density over each basin. Hence, in molecules, the integration of the electron density over a basin yields the average number of electrons on this basin. In particular, for a basin labelled Ω_A, its average number of electrons or electron population is given by

$$\tilde{N}(\Omega_A) = \int_{\Omega_A} \rho(\vec{r}) \mathrm{d}r. \tag{11}$$

Therefore, one expects that this number closely correlates with the empirical chemical knowledge about the number of electrons participating in a bond. For example, for the water molecule, the basin associated with the oxygen core has an average electron population of 2.08 electrons. The basins associated with the oxygen–hydrogen bonds have an average electron population of 1.78 and, finally, the basins associated with the electron lone pairs have an average electron population of 2.18. It is important to remember that this is only an average which has a quantum uncertainty. The uncertainty is given by the variance or fluctuation of the population. It is defined as

$$\sigma^2(\tilde{N}, \Omega_A) = < N^2 >_{\Omega_A} - < N >^2_{\Omega_A}, \tag{12}$$

where N represents the electron number operator and the brackets $< >_{\Omega_A}$ mean an integration over the volume of the basin. Since N^2 is a bielectronic operator one cannot evaluate the average using only the density. It is necessary to use the second-order density matrix. The quantity σ^2 was investigated by Bader in the context of the atoms in molecules model[48] and by Savin et al. in the context of the ELF.[45] The fluctuation σ^2 is an extensive quantity, and, therefore, it depends on the number of atoms of the system making difficult the comparison among molecules with different number of basins. Hence, it is convenient to introduce the relative fluctuation[48]

$$\lambda(\Omega) = \frac{\sigma^2(\tilde{N}, \Omega)}{\tilde{N}(\Omega)}, \tag{13}$$

which is a positive quantity and lower than one. An analysis of the electron delocalization based on the definition of a covariance operator has been recently discussed by Silvi, both in the AIM and in the ELF frameworks.[49]

Another useful concept of topological theory, which can help in quantifying the information carried on the basins, is the concept of *bifurcation*. At very low values of the ELF, you have only one *f-domain* which is reducible (it contains more than one

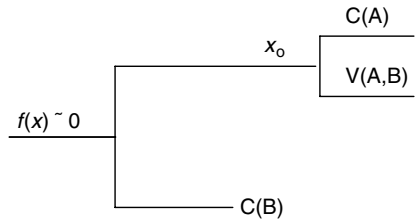

Figure 4 Bifurcation diagram of $f(x)$

attractor), and you will look at just one surface containing all the system. Increasing the value of the ELF, at the point of the minima, the basins separate and more than one *f-domain* appears. This is called a bifurcation, and it is clearly visualized by a bifurcation diagram like the one in Figure 4. This is the bifurcation, diagram of the function depicted in Figure 3. The first bifurcation corresponds to the separation of the disynaptic basin and the core basin of point B and occurs at the global minimum of the function. The second bifurcation appears later on and corresponds to the separation of the central disynaptic basin and the core basin associated with the point A. Hence, the points of bifurcation correspond to the minima of the function. In the case of the ELF, the lower the bifurcation point the more localized are the corresponding basins.

This kind of analysis based on bifurcations is connected to the concept of synaptic order previously defined,[47,49] and it has been applied to the study of electron localization in some simple chemical systems[45] as it will be noted below. A recent application showing the usefulness of this type of analysis has been reported by Silvi concerning the bonding nature of the VOx and VO$x+(x=1-4)$ molecular systems.[50]

2.7. Other developments

Topological analysis of the ELF constructed from density components has also been evaluated. Separations of the α–β spin[41,51] and the σ–π[52] electron contributions to density have been recently reported. Although the total ELF is not recovered by the addition of the individual components, the separation is a useful tool to evaluate some important electronic aspects of different classes of chemical systems as radicals or aromatic species.

The separation of spin components has been used to evaluate the radical characteristics of aromatic chemical systems.[51] The topological analysis was made over a separated density constructed from the α and β components. In this way, it was possible to visualize the degree of localization of the unpaired electron mainly in open-shell systems (see Figure 5). Hence, the α and β spin separation of the ELF provides more insights into chemical bonding structure. In particular, the ELF_α provides a qualitative description of the space region where is most probable to find an unpaired electron.[51] As an example, Figure 5 shows the ELF_α and ELF_β for the *para*-benzine radical in its singlet and triplet states which are known to be very near in energy. The *para*-benzine system has a particularly selective bioactivity and has been widely exploited for anticancer drug design.[53] Further, from a purely theoretical point of view the *para*-benzine system is a challenge to current calculation methods. The system undergoes a spatial symmetry

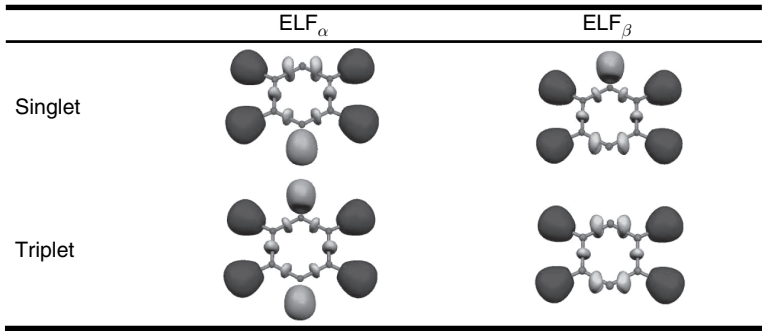

Figure 5 ELF isosurfaces of the *para*-benzine in singlet and triplet states

breaking, which means that the wave function obtained from standard single-determinant methods fails to transform as an irreducible representation of the molecular point group. Crawford et al. published a thorough study on this problem.[54] From Figure 5 one can see that the ELF$_\alpha$ and ELF$_\beta$ are different. One electron with spin α is located on the carbon atom at the bottom, whereas the other electron with β spin appears to be located on the carbon atom at the top of the figure.

Of course, this is an artifact of the calculation because the probability of having an electron with α and β spin is the same. Kraka et al.[55] demonstrated that the on-top density discussed by Perdew et al.[56] is able to reproduce the correct symmetry of the Hamiltonian.

In the same way as the α, β-separation has been performed, one can proceed to a σ, π-separation.[52] This separation has been used to evaluate the aromaticity of organic molecules and clusters. An index of aromaticity was proposed using a scale based on the bifurcation analysis of the ELF constructed from the separated densities. In principle, the total ELF has no information about π and σ bonds, it depends only on the total density. Hence, the ELF does not show clear differences between both kinds of bonds. However, the topological analysis over separated densities, ones formed by the π-orbitals and the other ones formed by the σ-orbitals, yields the necessary information.[52] Of course, this is possible only for the molecules which present the σ, π symmetries, i.e. planar molecules. The bifurcation analysis of the news ELF$_\pi$ and ELF$_\sigma$ can be interpreted as a measure of the interaction among the different basins and chemically, as a measure of electron delocalization.[45] In this way, the π and σ aromaticity for the set of planar molecules described in the Scheme 1 has been characterized.[52]

The aromatic rings present the highest and the antiaromatic systems the lowest bifurcation values of ELF$_\pi$. The bifurcation of the ELF$_\sigma$ occurs close to 0.75, except in system where sigma delocalization exists. In this way, the aromaticity of polycyclic aromatic hydrocarbons was well predicted, and also the aromaticity of new molecules was corroborated. In the all-metal aromatic compound Al_4^{2-} important contributions to stability from the two π aromatic electrons and the σ system in the plane of the molecule were observed. The isosurfaces of the total ELF, ELF$_\pi$ and ELF$_\sigma$ functions are showed in the Figure 6.

By this way, one can predict the existence of σ or π aromaticity, but it is difficult to predict the net aromaticity of species that presents σ aromaticity and π antiaromaticity at the same time as it occurs in systems like Al_4^{4-}. In this case, the average value of the

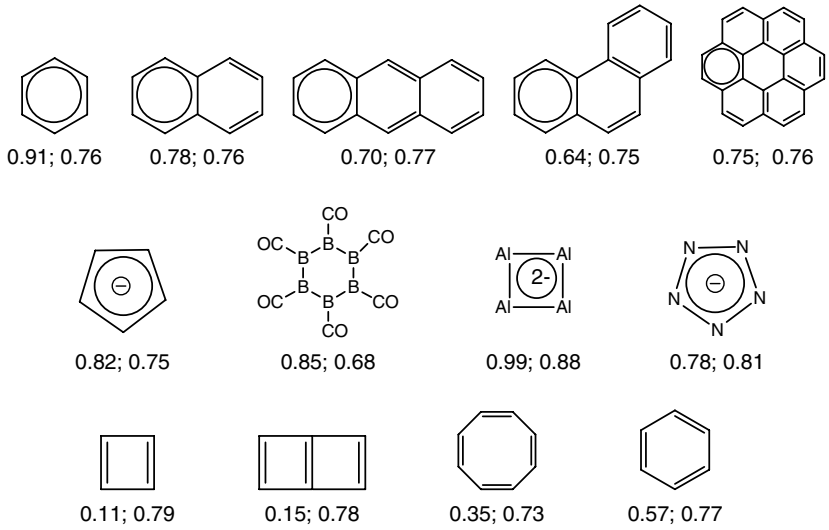

Scheme 1 Bifurcation values of ELF_{π} and ELF_{σ} functions for some aromatic and antiaromatic molecules

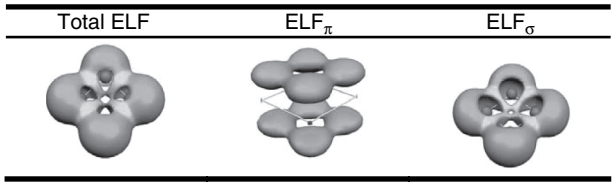

Figure 6 ELF isosurfaces of Al_4^{2-} cluster

ELF_{σ} and ELF_{π} bifurcations was used to construct a general scale to measure the global aromatic character of a molecular system.[57] This general scale predicted the electron delocalization characteristic of known organic and metallic aromatic and antiaromatic systems.

On a different development, recently an extension of the ELF to the time-dependent density functional formalism has been presented.[58] With the advent of attosecond laser pulses, the information of the time scale and temporal order of the different bond breaking or bond formation processes will be important, and this is the kind of information one can extract from the time-dependent version of the ELF.

3. Some applications

3.1. Molecular geometry and bond types

One of the first and most direct applications of the ELF is to the explanation and confirmation of the VSEPR model of Gillespie.[28] This was first done by Savin et al.[10] In molecular systems rich in electrons, the molecular distribution of the pairs of electrons

ab_2	$BeCl_2$	
ab_3	BCl_3	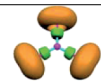
ab_4	CH_4	
ab_5	PCl_5	
ab_6	SCl_6	
ab_3e	NH_3	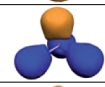
ab_2e_3	$XeCl_2$	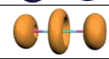
ab3e2	ClF_3	
ab4e	SF_4	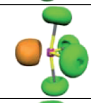
ab5e	BrF5	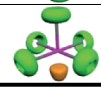

Figure 7 ELF isosurfaces for some molecules with typical geometries predicted by VSEPR model.

(lone and bonding) predicted by the VSEPR method can be visualized by means of the topological description of the ELF (see Figure 7). The classical representation of systems without lone pairs in the central atom (ab_x, $x = 2$–6) is very clear. In the systems with lone pairs on the central atom, it is important to appreciate the antiposition of the ELF attractors in molecules of type ab_3e_2, which is more distinctive than the VSEPR model. In molecules with three lone electron pairs at the central atom (ab_2e_3), the attractors are cylindrical in shape. There are also other studies of special molecules like the hexafluoride of xenon and related molecules.[59] The relevance of the octet rule in hypervalent molecules in the context of the ELF has been also studied.[60] Indeed, the molecules that present a non-VSEPR geometry have been also rationalized by means of the ELF.[61]

The typical kind of bonding in organic molecules can be easily seen in Figure 8. The C−H simple bond is represented by a disynaptic basin V(C,H) in blue colour. The C−C simple bonds are described by a circular region (green colour) between two core regions (violet colour). The C−C double bond is shown as a double region perpendicular to the line joining the atoms, and the attractors corresponding to C−C triple bond are distributed in a cylindrical shape. The two lone pairs of electrons in the oxygen atoms are clearly in antiposition as was commented before for systems ab_xe_2.

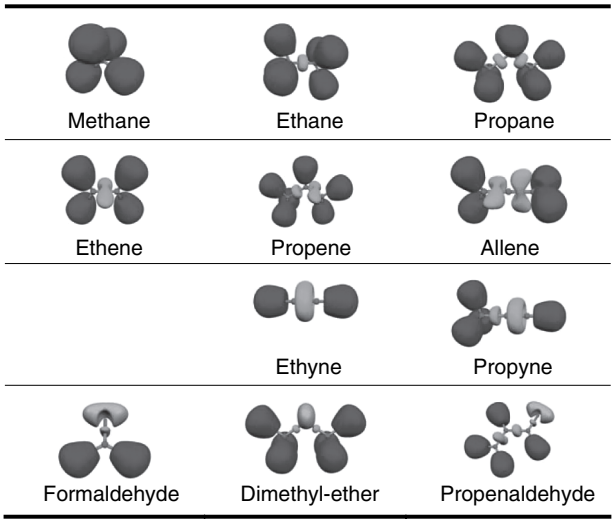

Figure 8 ELF isosurfaces of some classical organic molecules

The ELF is not only used to explain or to visualize the type of bond in the well-known molecules. It is also useful to clarify the type of bond in new molecules. For instance, it has been found that the new Na_SN_2 material has all the characteristics of a Zintl phase,[62] that the phase transition in iodine under compression is due to the presence of the lone pairs,[63] that the magnetic cluster Fe_4 is characterized by a large delocalization of the electron density[64] and that the contribution to bonding from the *d* electrons in the iridium atom in the new material $IrGa_2$ is important.[65] The localization nature of bonding at the superconducting stannide SrSn4 has been also explained, just like the homonuclear multiple bond between main group elements other than carbon, in particular the possible existence of a Ga–Ga triple bond in some new complexes.[66]

3.2. The nature of pericyclic and pseudopericyclic bonding at concerted transition states

ELF analysis has been probed to be a powerful scheme to elucidate between the pericyclic and pseudopericyclic character of bonding at concerted transition states. In this context, ELF methodology has been recently applied to get new insights concerning the nature of bonding at the transition states of the thermal electrocyclization of (*Z*)-1,2,4,6-heptatetraene ($X{=}CH_2$) and its heterosubstituted analogues, (2Z)-2,4,5-hexatrienal (X═O) and (2Z)-2,4,5-hexatrien-1-imine (X═NH) (see Scheme 2).[67]

It is known that a pseudopericylic pathway is characterized by the lack of cyclic orbital overlap, that is, there exists one or more *disconnections* in the bonding along the cyclic array of interacting centres.[68,69] Other characteristics which make interesting these type of reactions are that they have nearly planar and no anti-aromatic transition states, providing low activation barriers. On the other hand, pericyclic reactions involve no disconnection in the cyclic array of overlapping orbitals, non-planar allowed or forbidden transition states (depending on the number of electrons) with characteristic activation

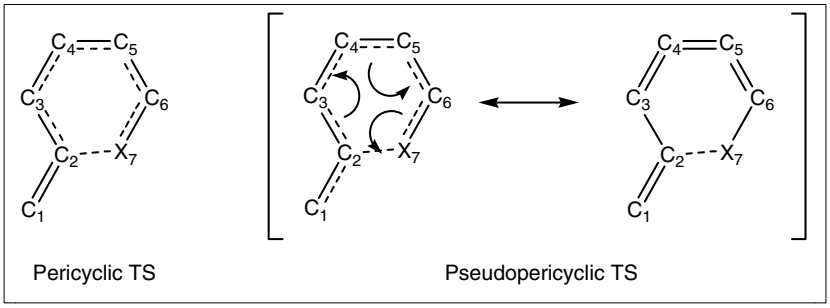

Scheme 2 Transition structures for the thermal electrocyclization of (Z)-1,2,4,6-heptatetraene (X=CH_2) and its heterosubstituted analogues, (2Z)-2,4,5-hexatrienal (X=O) and (2Z)-2,4,5-hexatrien-1-imine (X=NH)

energy barriers.[69] In the present case,[67] ELF results provide further evidence in support of a single disrotatory pericyclic interaction for the X=NH, X=O and X=CH_2 cases. This conclusion is based on the fluctuation analysis of electron density (i.e. covariance contributions interpreted in terms of *delocalization*) at the cyclic reaction centre upon the formation of the new C2−X7 bond. The fluctuation pattern is found to be very similar in the three cases. Furthermore, it is found that lone pair populations when X=NH and X=O are lower than 5%, and it seems to play, as suggested first by Rodriguez-Otero and Cabaleiro-Lago,[70] only a stabilizing role in the global electrocyclization process. These findings based on ELF analysis contribute to the relevant controversy concerning the pericyclic or pseudopericyclic intimate nature of bonding at these heterocyclic transition structures (TSs).[71,72]

It has also been previously shown[73] that the fluctuation pattern of electron density in the ELF basins provides a consistent description of pseudopericyclic and pericyclic bonding in concerted processes such as thermal chelotropic decarbonilation reactions.[74] Experimental support for planar pseudopericyclic transition states in chelotropic decarbonilations has been recently reported.[75] ELF picture of bonding reveals that for the eight transition states analysed (see Scheme 3), the departing CO can be visualized in terms of a carbon monoxide structure with a 'lone pair' region on the carbon atom.

Based upon the average bonding contributions (in per cent) to the 'lone pair' region centred at the carbon atom of the CO-leaving group and bifurcation diagrams, a clear distinction between the pseudopericyclic and pericyclic topologies can be achieved. Henceforth, this type of covariance analysis based on the ELF topology could constitute a complementary value to the traditional Woodward–Hoffmann symmetry-orbital rules.[76]

3.3. The ELF and the chemical bonding along reaction processes

Some of the concepts of the catastrophe theory[77] have been recently invoked in connection with ELF topological analysis to study the changes of bonding characteristics along chemical processes. In this context, Krokidis and co-workers have investigated the ammonia inversion, the breaking of the ethane C−C bond, and the breaking of the dative bond in NH_3BH_3,[78] the proton transfer in malonaldehyde,[79] the proton transfer in the protonated water dimmer,[80] the isomerization mechanisms in XNO (X=H, Cl),[81]

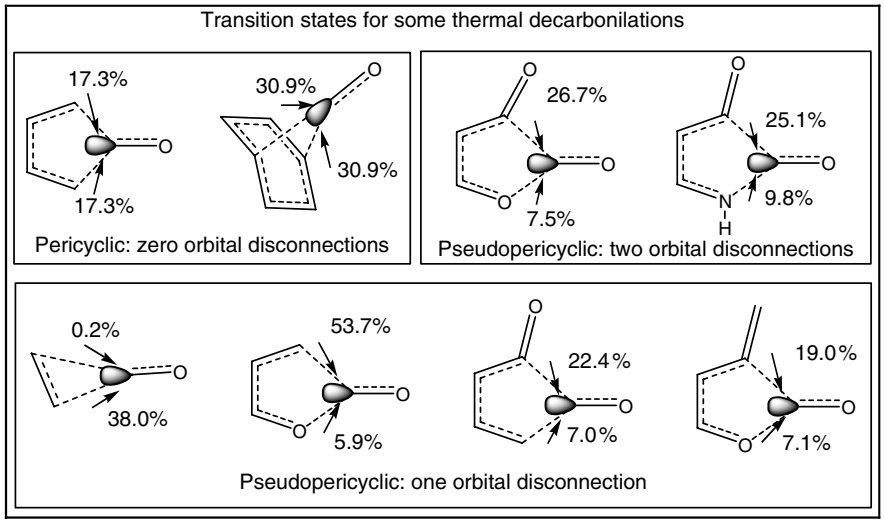

Scheme 3 Analysis of the pericyclic and pseudopericyclic nature of bonding for some thermal decarbonilations

and more recently the nature of the electron transfer and three-electron bonding in the reaction of Li with Cl_2.[82]

The nature of the change in chemical bonding along the reaction coordinate of some simple pericyclic reactions has been also explored.[83] For instance, ELF analysis has been found useful for describing the bond breaking/bond forming at concerted transition states. In particular, a concerted antarafacial bonding nature for the [1s,3a]hydrogen, a biradical interaction for the [1a,3s]methyl and an ionic interaction for the [1a,3s]fluorine sigmatropic rearrangements in the allyl system (see Scheme 4) have been fully characterized through the examination of integrated densities over the ELF basins and their related variance properties.

On the one hand, the fluctuation of electron density forms a cyclic and characteristic antarafacial pattern of bonding in the first case, while on the other, monosynaptic

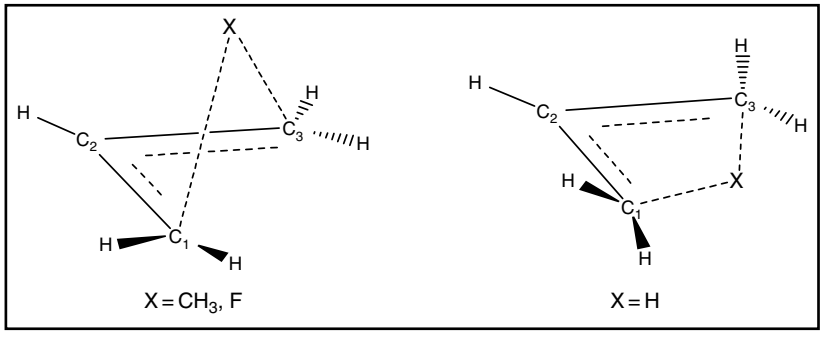

Scheme 4 [1s,3a]hydrogen, [1a,3s]methyl and [1a,3s]fluorine sigmatropic rearrangements in the allyl system. ELF analysis reveals a concerted interaction in the first case, a biradical interaction in the second one and a ion-pair interaction in the last one

basins, localizing approximately one electron, have been found on the methyl and allyl fragments. In the case of the fluorine migration, the ELF basin structure allows us to determine a charge separation of 0.6e between negative-charged fluorine and a positive allyl fragment. A deeper understanding of these molecular reaction mechanisms can thus be achieved in terms of the rearrangement of electron density among the ELF basins.

The [1a,3s] sigmatropic shift of the fluorine atom in the 3-fluorpropene system has been also previously discussed in detail. The transition state has been thoroughly characterized in terms of a ion-pair structure with a charge separation of 0.6e, and the changes in the bonding characteristics along the intrinsic reaction coordinate reaction (IRC) path (see Schemes 5a and 5b) were described in terms of the ELF basin properties, i.e. electron populations, variance and delocalization indexes.[84]

We would also like to mention here that ELF analysis has been also found valuable into the detailed description of intramolecular proton-transfer reactions in some thiooxalic acid derivatives HY-C(=O)-C(S)-XH, (1) X=O, Y=O; (2) X=O, Y=S; (3) X=S, Y=S, depicted in Scheme 6.[85]

In all these cases, ion-pair transition structures have been characterized, and the intimate nature of bonding has been discussed using the electron properties arising from ELF analysis. In particular, charge separations of 0.48e, 0.42e and 0.18e can be deduced from the basin structure and populations for the oxygen to oxygen, sulfur to oxygen and sulfur to sulfur proton-transfer transition states, respectively.

3.4. Reactions yielding aromatic products

3.4.1. Radical reactions: Bergman reaction

The reaction mechanism of the Bergman cyclization of the (Z)-hexa-1,5-diyne-3-ene to yield *p*-benzyne (Scheme 7 and Figure 9) has been studied recently in the framework

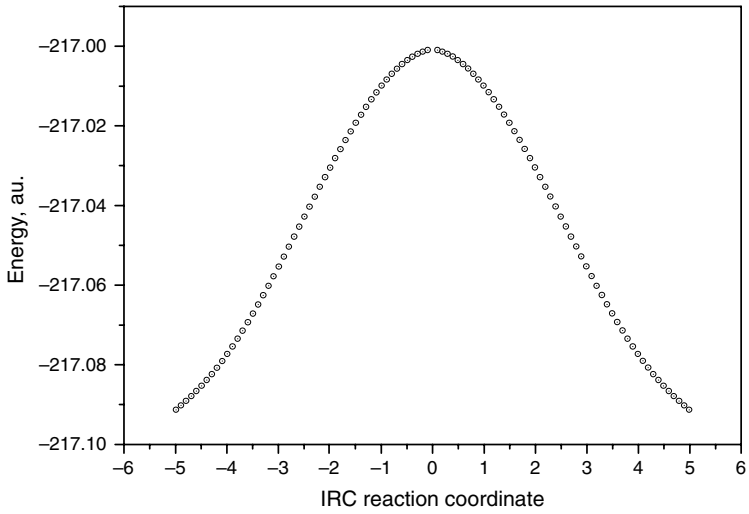

Scheme 5a Total energy along the IRC for the [1a,3s]F sigmatropic shift

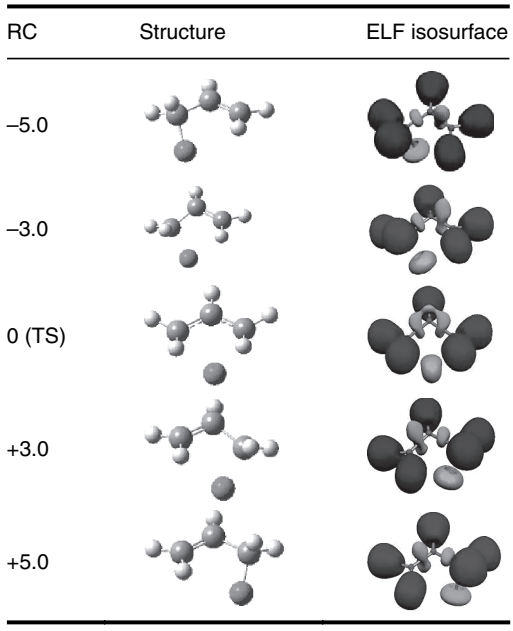

Scheme 5b ELF isosurfaces of some selected points of IRC

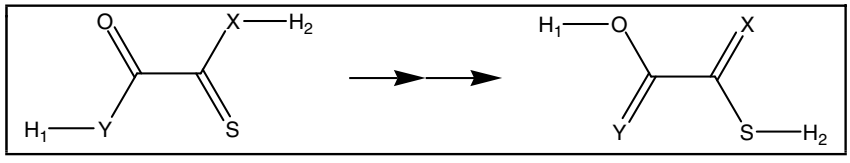

Scheme 6 Proton transfer of thiooxalic acid derivatives

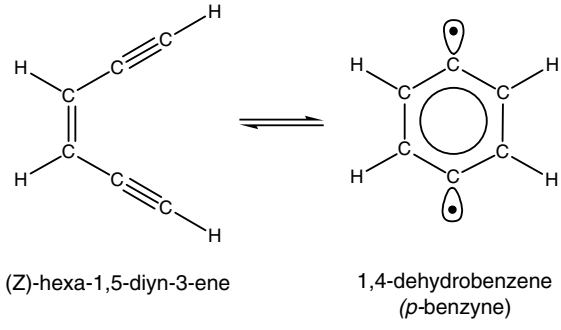

Scheme 7 Bergman reaction of (Z)-hexa-1,5-diyne-3-ene

of the ELF.[86] In this study, the evolution of the bonding along the reaction path is modelled by the changes in the number and synaptic order of the ELF valence basins, and each topological configuration comprised a structural step or stability domain.

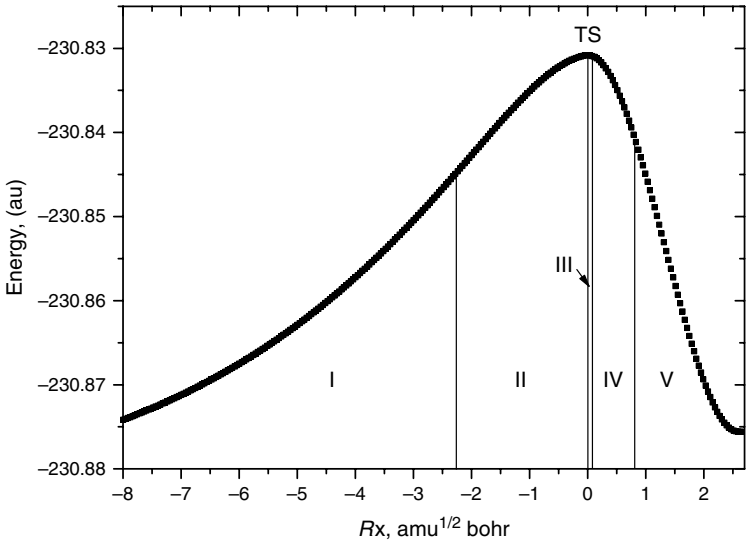

Figure 9 IRC profile of the Bergman cyclization of (Z)-hexa-1,5-diyn-3-ene

Five domains of structural stability of the ELF along the intrinsic reaction path were determined. The first is the most costly in terms of energy, and it presents strongly geometry changes with small variations in the population of ELF basins. In the second step appears two monosynaptic basins V(C2) and V(C5) in the backside of C_2 and C_5, enhancing the biradicaloid character of the moiety. The TS or third step shows a strong electron rearrangement with participation for the first time of the double bond C_3–C_4. In step IV, two monosynaptic basins are created on C_1 and C_6 atoms by electron transfer from the initial triple bonds basins as a prelude to cyclization. In this step, characteristics of biradical system are appreciated. The last step corresponds to the closure of the ring by the formation of a disynaptic basin $V(C_1, C_6)$ to reach the electronic characteristics of the *p*-benzyne. The ELF basin isosurfaces of the steps described before are depicted in Figure 10. In addition, the separation of the ELF into in-plane (ELF_σ) and out-of-plane (ELF_π) contributions allowed discussing the aromaticity profiles (see Figure 11). σ aromaticity appears in the vicinities of the TS, and it is provided exclusively by the delocalization of the in-plane electronic system, while π aromaticity takes place in the final stage of the reaction path, once the ring has been formed, being maximum in the *p*-benzyne.

A related study but concerning the 1,3-dipolar cycloaddition of fulminic acid and ethyne was previously reported.[87]

3.4.2. Trimerization of acetylene

The reaction mechanism and the development of the aromaticity along the trimerization of acetylene to yield benzene (Scheme 8, Figure 12) have been analysed by the ELF in the same framework of structural stability domains described before.[88]

The electronic rearrangements associated with bond breaking/forming processes determined five steps along the intrinsic reaction path, the ELF isosurfaces that characterized

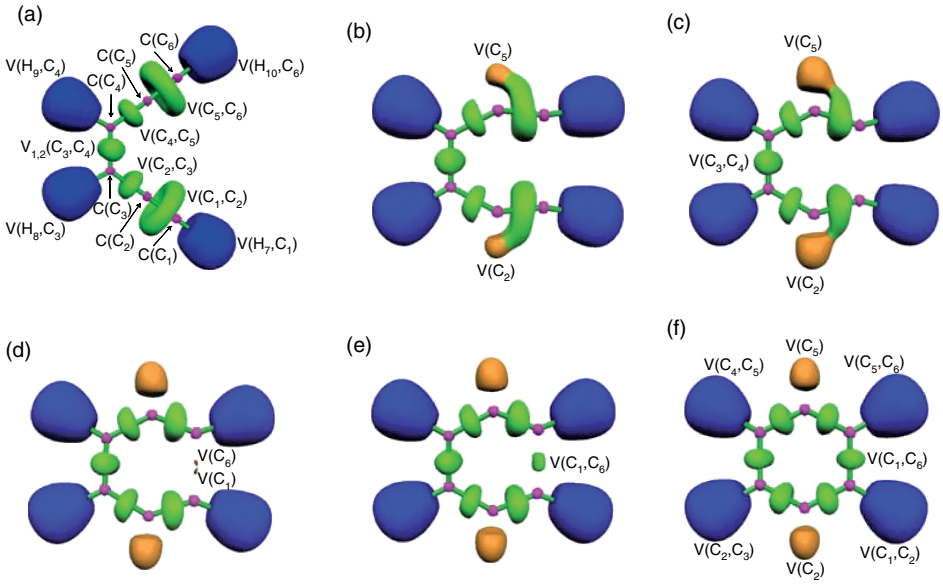

Figure 10 ELF isosurfaces for: (a) (Z)-hexa-1,5-diyn-3-ene, (b) step II, (c) step III (TS), (d) step IV, (e) step V and (f) *p*-benzyne

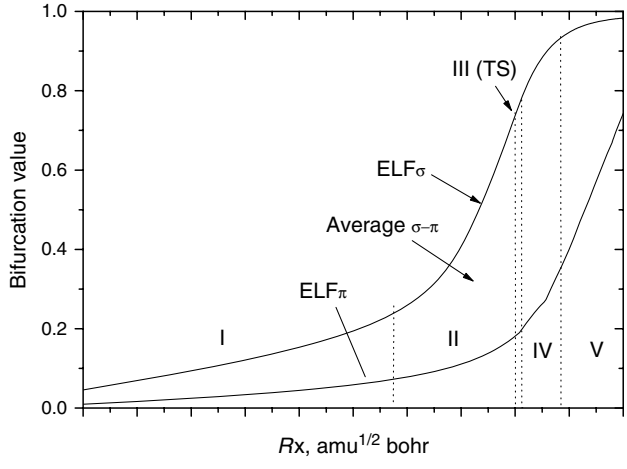

Figure 11 Evolution of the ELF_{σ}, ELF_{π} and average ELF_{σ}–ELF_{π} along the IRC path of Bergman cyclization

each step are shown in the Figure 13. In the first step, there is an approximation between acetylene moieties without rearrangement of electron density between ELF basins. In step II, which includes the TS, each valence basin corresponding to a triple bond is transformed into two degenerate basins out of plane of the molecule. This

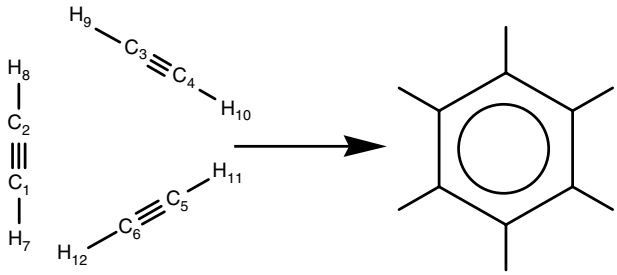

Scheme 8 Trimerization of acetylene

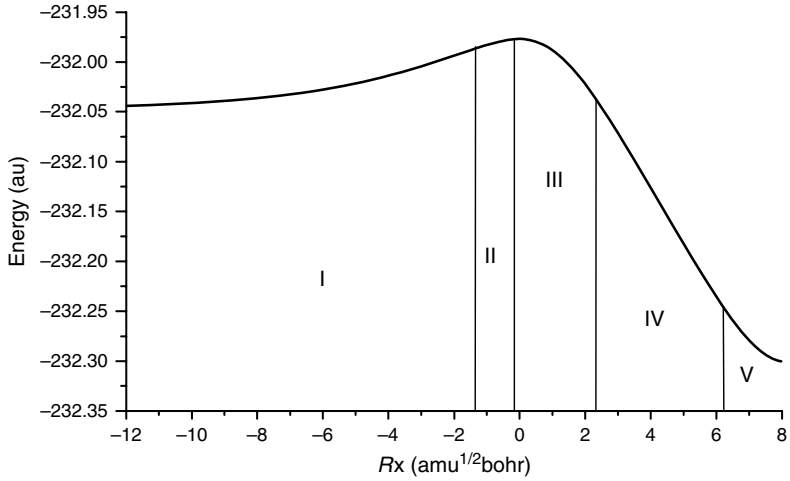

Figure 12 IRC profile of the trimerization of acetylene

step is characterized by the deformation of the acetylene units in order to reduce the closed-shell repulsive interaction. Step III corresponds to the simultaneous formation of a monosynaptic basin over each carbon atom preparing for the cyclization of the system. In the fourth step occurs the formation of a six-membered cycle, associated with the formation of three disynaptic basins representing new C–C covalent bonds. In the last step, the three pairs of disynaptic basins are transformed into monosynaptic basins, and the valence basin populations are equalized resembling the transformation of non-aromatic into aromatic benzene.

The analysis of in-plane (ELF_σ) and out-of-plane (ELF_π) contributions (Figure 14) shows that the TS has a low σ-electron delocalization which is assigned to a process of through-space electron delocalization without π-aromatic character. At the end of step IV, ELF_π increases sharply while ELF_σ decreases slowly, according with the beginning of diatropic π current as was previously observed by the analysis of magnetic properties.[89] The increase of ELF_π bifurcation values in this step of the reaction does not reveal aromaticity according to the separated ELF scale. The π aromaticity only is developed at the final stage of the reaction.

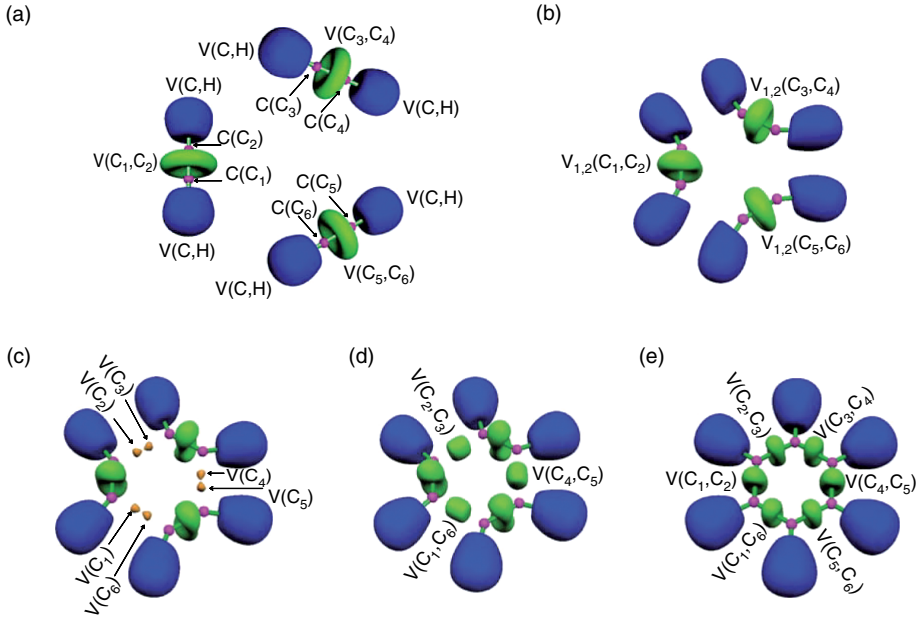

Figure 13 ELF isosurfaces for: (a) acetylenes moieties, (b) step II (TS), (c) step III, (d) step IV and (e) step V (benzene)

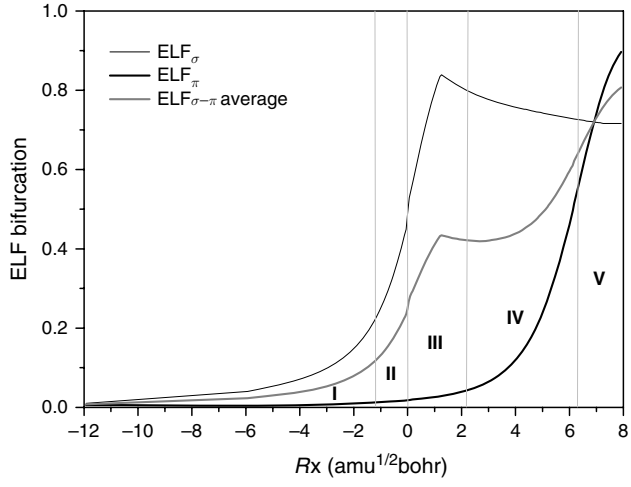

Figure 14 Evolution of the ELF$_\sigma$, ELF$_\pi$ and average ELF$_\sigma$–ELF$_\pi$ along the IRC path of trimerization of acetylene

3.5. Applications to atomic clusters

The atomic clusters are defined as a conglomerate of atoms from as few as two to hundreds of them. They are usually produced by evaporation of the metal, and most of them are highly reactive. Hence, most of them exist only in gas phase. One of

the most known exceptions is the fullerene, which is so stable that crystallize easily. Besides its importance in the nanotechnology, they are from a theoretical point of view interesting due to the variety of bonding they present. For instance, the magnesium dimer, the smallest magnesium cluster, presents a van der Waals type of bonding, the bigger clusters, say Mg_{10}, present a covalent bond and when the cluster is growing at same point the bond should be metallic in character like the solid. To elucidate the type of bonding in clusters, the ELF is of high utility. It is important to notice that most of them do not follow the Lewis rules of bonding, and they are not described by a simple Lewis structure. For instance, think on the Li_4 cluster. On the ground state, it is a rhombus. Hence, each lithium atom is surrounded by two other lithium atoms, and there are four valence electrons to bind all the atoms. It is impossible to draw a Lewis structure. In Figure 15, one can see an ELF isosurface for Li_4. There are two valence basins surrounding three lithium atoms each. The population of each basin is of around 2e. Therefore, the picture is very clear. The Li_4 cluster is held together through two two-electron-three-centre bonds. In an exhaustive work, Rousseau and Marx[90] used the ELF to understand the variations in the type of bonding of lithium clusters, nanoclusters, bulk metal and surfaces. They concluded that the electrons prefer to localize in the interstitial regions, leading to multicentre bonding for both the clusters and the solids, including their surfaces. For nanoscale clusters (Li_{40}), only the surface presents strong localization and the interior displays localization properties similar to the bulk metallic solid.

The ELF not only permits to understand the type of bonding but also to do some predictions about the reactivity of the clusters.[91] Taking again Li_4 as an example, one can try to predict at which position will a hydrogen atom bind to the cluster, on top of a lithium atom, in a bridge position between two atoms or from above the four atoms?. The hydrogen atom is more electronegative than a lithium atom. Therefore, the hydrogen atom will take charge from the cluster, and the bond will be polar. Hence, it is reasonable to think that the hydrogen atom will approach the cluster on the regions where it is most probable to find the valence electrons. Looking at the ELF isosurface, one can predict that the hydrogen atoms will attach to the cluster at a bridge position between two lithium atoms. In Figure 15 one can see an ELF isosurface for the hydrogenated cluster of Li_4H_2. Each hydrogen basin has a population of 2e and the two-electron-three-centre basin at the top of the figure remains with a population of around 2e. Note that the cluster is divided into two regions, one with delocalized electrons and one with localized electrons, as should be in a model for a metallic–insulator interphase.

A special branch of the atomic cluster research is the study of clusters of the metal transition atoms, especially because of their catalytic properties. However, for the transition metal atoms, the application of the ELF deserves to be carefully analysed. One

Figure 15 ELF isosurface of Li_4 and Li_4H_2

observes two characteristic features in systems formed by transition metal atoms. The ELF presents very low values almost everywhere, and the number of attractors augments considerably. For instances, in a recent study of the ground state of Fe_4 the ELF analysis[64] reveals 21 attractors, and it presents always values lower than 0.5, the electron gas reference value. These two features obviously complicate the analysis.[92–94] Kohout et al. have carefully examined this point.[95]

4. Conclusions and outlook

Some general aspects related to the derivation, and interpretations of ELF analysis, as well as some representative applications have been briefly discussed. The ELF has emerged as a powerful tool to understand in a qualitative way the behaviour of the electrons in a nuclei system. It is possible to explain a great variety of bonding situations ranging from the most standard covalent bond to the metallic bond. The ELF is a well-defined function with a nice pragmatic characteristic. It does not depend neither on the method of calculation nor on the basis set used. Its application to understand new bond phenomenon is already well documented and it can be used safely. Its relationship with the Pauli exclusion principle has been carefully studied, and its consequence to understand the chemical concept of electron pair has also been discussed. A point to be further studied is its application to transition metal atoms with an open d-shell. The role of the nodes of the molecular orbitals and the meaning of ELF values below 0.5 should be clarified.

Acknowledgements

Our thanks to Profs. A. Savin and B. Silvi (Paris) for introducing us to the world of the electron localization function. We acknowledge the support received from MIDEPLAN and CONICYT through the Millennium Nucleus for Applied Quantum Mechanics and Computational Chemistry, project P02-004-F. J.C.S. thanks Universidad Técnica Federico Santa Maria for the support through grant UTFSM 130423. E.C. is also grateful to Universidad Andrés Bello for the support received through the project UNAB DI 16-04. We finally thank Fondecyt for financial support through grant nos. 1030173 and 1050294.

References and notes

1. S. Zoury, X. Krokidis, F. Fuster and B. Silvi, Computers & Chemistry (Oxford) (1999) 23 597. See also: http://www.jussieu.fr/silvi
2. The oficial WEB site for this commercial software is http://www.gaussian.com
3. The General Atomic and Molecular Electronic Structure System (GAMESS): www.msg.ameslab.gov/GAMESS/GAMESS.html
4. For instance: **(a)** The Car-Parrinello Molecular Dynamics code (CPMD, http://www.cpmd.org/ http://www.cpmd.org/) implements an ELF for the valence electrons, both in a spin-polarized average of ELF as well as the separate α and β orbital contributions as it has been proposed by M. Kohut and A. Savin, Int. J. Quant. Chem. 60 (1996) 875; **(b)** The VASP package

(http://cms.mpi.univie.ac.at/CMSPage/main/) also implements the ELF in a framework of mechanical molecular dynamics (MD) using pseudopotentials and a plane wave basis set.
5. Utility program written by M. Kohout, Max Planck Institute for Chemical Physics of Solids, Dresden, Germany. For contact and to obtain the program, please E-mail to: kohout@cpfs.mpg.de with the Subject: DGrid
6. The official WEB site for this commercial software is: http://www.molpro.net/
7. The official WEB site for this commercial software is: http://www.scm.com/
8. P. Soler, F. Fuster and H. Chevreau, J. Comput. Chem. 25 (2004) 1920
9. A. D. Becke and K. E. Edgecombe, J. Chem. Phys. 92 (1990) 5397
10. A. Savin, R. Nesper, S. Wengert and T. Fassler, Angew. Chem. Int. Ed. Engl. 36 (1997) 1808
11. B. Silvi and A. Savin, Nature 371 (1994) 683
12. W. Pauli, Z. Physik 36 (1926) 336
13. G. N. Lewis, J. Am. Chem. Soc. 38 (1916) 762
14. R. F. W. Bader, Atoms in Molecules. A Quantum Theory, Clarendon Press, Oxford, 1990
15. Y. Tal and R. F. W. Bader, Int. J. Quant. Chem. Quant. Chem. Symp. 12 (1978) 153
16. M. Kohout and A. Savin, Int. J. Quant. Chem. 18 (1997) 1431
17. V. Tsirelson and A. Stash, Chem. Phys. Lett. 351 (2002) 142
18. S. R. Gadre, S. A. Kulkarni and R. K. Pathak, J. Chem. Phys. 98 (1993) 3574
19. P. Fuentealba, Int. J. Quant. Chem. 69 (1998) 559
20. P. K. Chattaraj, E. Chamorro and P. Fuentealba, Chem. Phys. Lett. 314 (1999) 114
21. P. Ayers, R. Parr and A. Nagy, Int. J. Quant. Chem. 90 (2002) 309
22. M. Kohout, K. Pernal, F. Wagner and Y. Grin, Theor. Chem. Acc. 112 (2004) 453
23. A. Savin, H. J. Flad, J. Flad, H. Preuss and H. G. von Schnering, Angew. Chem. 104 (1992) 185
24. C. Von Weizsacker, Z Phys 96 (1935) 431
25. A. Burckhardt, U, Wedig, H, G. von Schnering and A. Savin, Z. Anorg. Allg. Chem. 619 (1993) 437
26. F. Zurcher, S. Leoni and R. Nesper, Z. F. Kristalog. 218 (2003) 171
27. J. K. Burdett and T. A. McCornick, J. Phys. Chem. A102 (1998) 6366
28. R. J. Gillespie, Molecular Geometry, van Nostrand Reinhold, London, 1972; R. J. Gillespie and R. S. Nyholm, Rev. Chem. Soc. 11 (1957) 239
29. R. F. W. Bader, S. Johnson, T. H. Tand and P. L. A. Popelier, J. Phys. Chem. A 100 (1996) 15398
30. R. F. W. Bader and G. L. Heard, J. Chem. Phys. 111 (1999) 8789
31. R. Llusar, A. Beltran, J. Andres, F. Fuster and B. Silvi, J. Phys. Chem. A105 (2001) 9460
32. D. B. Chesnut and L. J. Bartolotti, Chem. Phys. 257 (2000) 175
33. S. Roggan, G. Schnakenburg, C. Limberg, S. Sandhoefner, H. Pritzkow and B. Ziemer, Chem. Eur. J. 11 (2004) 225
34. J. J. Panek, A. Jezierska, K. Mierzwicki, Z. Latajka and A. Koll, J. Chem. Inf. Comp. Sci. 45 (2005) 39–48.
35. (a) A. Bil and Z. Latajka, Chem. Phys. 305 (2004) 243 (b) A. Bil and Z. Latajka, Chem. Phys. 303 (2004) 43
36. J. R. Sambrano, L. Gracia, J. Andres, S. Berski and A. Beltran, J. Phys. Chem. A 108 (2004) 10850
37. J. R. B. Gomes, F. Illas and B. Silvi, Chem. Phys. Lett. 388 (2004) 132
38. J. Pilme, B. Silvi, M. E. Alikhani, J. Phys. Chem. A 107 (2003) 4506
39. J. Boily, J. Phys. Chem. A 107 (2003) 4276
40. J. Molina and J. A. Dobado, Theor. Chem. Acc. 105 (2001) 328
41. M. Kohout and A. Savin, Int. J. Quant. Chem. 60 (1996) 875.
42. R. J. Boyd, Can. J. Phys. 56 (1978) 780.
43. A. M. Simas, R. P. Sagar, A. C. Ku and V. H. Smith Jr., Can. J. Chem. 66 (1988) 1923.

44. M. Kohout and A. Savin, Int. J. Quant. Chem. 18 (1997) 1431.
45. A. Savin, B. Silvi and F. Colonna, Can. J. Chem. 74 (1996) 1088.
46. S. Noury, F. Colonna, A. Savin and B. Silvi, J. Mol. Struct. 450 (1998) 59
47. B. Silvi, J. Mol. Struct 614 (2002) 3
48. R. F. W. Bader, in Localization and Delocalization in Quantum Chemistry, vol. 2. Edited by O. Chalvet et al. Reidel, Dordrecht, 1976
49. B. Silvi, Phys. Chem. Chem. Phys. 6 (2004) 256
50. M. Calatayud, J. Andres, J. Beltran and B. Silvi Theor. Chem. Acc. 105 (2001) 299
51. J. Melin, P. Fuentealba, Int. J. Quant. Chem. 92 (2003) 381
52. J. C. Santos, W. Tiznado, R. Contreras, P. Fuentealba, J. Chem. Phys. 120 (2004) 1670
53. K. C. Nicolau, A. L. Smith, S. Wendeborn and C. K. Wang J. Am. Chem. Soc. 113 (1991) 3106
54. T. D. Crawford, E. Kraka, J. F. Stanton and D. Cremer, J. Chem. Phys. 114 (2001) 10638
55. J. Grafenstein, A. Hjerpe, E. Kraka and D. J. Cremer, J. Phys. Chem. A104 (2000) 1748
56. J. P. Perdew, A. Savin and K. Burke, Phys. Rev. A51 (1995) 4531
57. J. C. Santos, J. Andres, A. Aizman and P. Fuentealba, J. Chem. Theory Comput. 1 (2005) 83
58. T. Burnus, M. A. L. Marquez and E. K. U. Gross, Phys. Rev. A 71 (2005) 10501
59. Y. Simon-Manso and P. Fuentealba, Theochem 634 (2003) 89
60. S. Noury, B. Silvi and R. J. Gillespie, Inorg. Chem. 41 (2002) 2164
61. R. J. Gillespie, S. Noury, J. Pilme and B. Silvi, Inorg. Chem. 43 (2004) 3248
62. F. Dubois, M. Schreyer and T. F. Fassler, Inorg. Chem. 44 (2005) 477
63. A. Savin J. Phys. Chem. Solids 65 (2004) 2025
64. S. Berski, G. Gutsev, M. Mochena and J. Andres, J. Phys Chem. A 108 (2004) 6025
65. M. Bostrom, Y. Prots and Y Grin, Solid State Sci. 6 (2004) 499
66. H. Grutzmacher and Th. Faessler, Chem. Eur. J. 6 (2000) 2317.
67. E. E. Chamorro and R. Notario, J. Phys. Chem. A. 108 (2004) 4099
68. J. A. Ross, R. P. Seiders and D. M. Lemal, J. Am. Chem. Soc. 98 (1976) 4325
69. See for instance: (a) D. M Birney, Org. Lett. 6 (2004) 85; (b) C. Zhou and D. M Birney, J. Org. Chem. Soc. 69 (2004) 86; (c) C. Zhou and D. M. Birney, J. Am. Chem. Soc. 125 (2003) 15268; (d) C. Zhou and D. M. Birney, J. Am. Chem. Soc. 124 (2002) 5231; (e) W. W. Shumway, N. K. Dalley and D. M. Birney J. Org. Chem., 66 (2001) 5832; (f) D. M. Birney, J. Am. Chem. Soc. 122 (2000) 10917; (g) D. M. Birney, X. L. Xu and S. Ham, Ang. Chem. Inter. Ed. Engl. 38 (1999) 189
70. J. Rodriguez-Otero and E. M. Cabaleiro-Lago Chem. Eur. J. 9 (2003) 1837
71. (a) A. R. De Lera, R. Alvarez, B. Lecea, A. Torrado and F. P. Cossio Ang. Chem. Inter Ed. Engl. 40 (2001) 557; (b) J. Rodriguez-Otero and E. M. Cabaleiro-Lago Angew. Chem., Int. Ed. 41 (2002) 1147; (c) A. R. De Lera, F. P. Cossio, Angew. Chem., Int. Ed. 41 (2002) 1150; (d) J. Rodriguez-Otero and E. M. Cabaleiro-Lago Chem. -Eur. J. 9 (2003) 1837
72. (a) E. Matito, M. Sola, M. Duran and J. Poater, Comment on the "Nature of Bonding in the Thermal Cyclization of (Z)-1,2,4,6-Heptatetraene and its Heterosubstituted Analogues" J. Phys. Chem. A (2005) in press. (b) E. E. Chamorro and R. Notario, J. Phys. Chem. A ("Reply to 'Comment on the "Nature of Bonding in the Thermal Cyclization of (Z)-1,2,4,6-Heptatetraene and its Heterosubstituted Analogues" J. Phys. Chem. B 109 (15) 7594–7595 (April 21, 2005)
73. E. Chamorro, J. Chem. Phys. 118 (2003) 8687
74. D. M Birney, S. Ham and G. R. Unruh, J. Am. Chem. Soc. 119 (1997) 4509
75. H. X. Wei, Z. Chun, S. Ham, J. M. White and D.M. Birney, Org. Lett. 6 (2004) 4289
76. (a) R. B. Woodward and R. Hoffmann J. Am. Chem. Soc. 87 (1965) 395; (b) R. Hoffmann and R. B. Woodward, J. Am. Chem. Soc. 87 (1965) 2046; (c) R. Hoffmann and R. B. Woodward, J. Am. Chem. Soc. 87 (1965) 4389; (d) R. Woodward and R. Hoffmann, Angew. Chem. Int. Ed. 8 (1969) 781

77. (a) R. Thom 1975. Structural Stability and Morphogenesis: An Outline of a General Theory of Models. London: Benjamin; (b) R. Thom 1983. Mathematical Models of Morphogenesis, Chichester: Horwood.; (c) R. Gilmore, Catastrophe Theory for Scientists and Engineers Dover Publications; Reprint edition (July 1, 1993); (d) P. T. Saunders, An Introduction to Catastrophe Theory. Cambridge University Press (June 30, 1980)
78. X. Krokidis, S. Noury and B. Silvi, J. Phys. Chem. A 101 (1997) 7277
79. X. Krokidis, V. Goncalves, A. Savin and B. Silvi, J. Phys. Chem. A 102 (1998) 5065
80. X. Krokidis, R. Vuilleumier, D. Borgis and B. Silvi, Mol. Phys. 96 (1999) 265
81. X. Krokidis, B. Silvi and M. E. Alikhani, Chem. Phys. Lett. 292 (1998) 35
82. X. Krokidis and A. Sevin, Progress in Theoretical Chemistry and Physics 2 (2000) (Quantum Systems in Chemistry and Physics, Vol. 1), 345
83. E. Chamorro, J. C. Santos, B. Gomez, R. Contreras and P. Fuentealba, J. Phys. Chem. A: 106 (2002) 11533.
84. E. Chamorro, J. C. Santos, B. Gomez, R. Contreras and P. Fuentealba, J. Chem. Phys. 114 (2001) 23
85. E. Chamorro, A. Toro-Labbe and P. Fuentealba, J. Phys. Chem. A 106 (2002) 3891
86. J. C. Santos, J. Andres, A. Aizman, P. Fuentealba and V. Polo, J. Phys. Chem. A 109 (16) (2005) 3687–3693
87. V. Polo, J. Andres, R. Castillo, S. Berski and B. Silvi, Chemistry-A European journal 10 (2004) 5165
88. J. C. Santos, V. Polo and J Andres, Chem. Phys. Lett 406 (4–6) (2005) 393–397
89. R. Havenith, P. Fowler, L. Jenneskens and E. Steiner, J. Phys. Chem. A 107 (2003) 1867
90. R. Rousseau and D. Marx, Chem. Eur. J. 6 (2000) 2982
91. P. Fuentealba and A. Savin, J. Phys. Chem. A 105 (2001) 11531
92. R. Llusar, A. Beltran, J. Andres, F. Fuster and B. Silvi, J. Phys. Chem. A105 (2001) 9460
93. Michelini, N. Russo, M. Alikhani and B. Silvi, J. Comput. Chem. 25 (2004) 1647
94. J. Pilme, B. Silvi and M. Alkhani, J. Phys. Chem. 107A (2003) 4506
95. M. Kohout, F. Wagner and Y. Grin, Theor. Chem. Acc. 108 (2002) 150